

RESEARCH ARTICLE

Specification of basal region identity after asymmetric zygotic division requires mitogen-activated protein kinase 6 in rice

Kiyoe Ishimoto^{1,*}, Shino Sohonahra¹, Mitsuko Kishi-Kaboshi^{2,‡}, Jun-ichi Itoh³, Ken-ichiro Hibara^{3,§}, Yutaka Sato^{4,¶}, Tsuneaki Watanabe^{2,**}, Kiyomi Abe^{2,‡}, Akio Miyao^{2,¶}, Misuzu Nosaka-Takahashi⁵, Toshiya Suzuki⁵, Nhung Kim Ta⁵, Sae Shimizu-Sato⁵, Takamasa Suzuki⁶, Atsushi Toyoda⁵, Hirokazu Takahashi¹, Mikio Nakazono¹, Yasuo Nagato³, Hirohiko Hirochika² and Yutaka Sato^{5,§§}

ABSTRACT

Asymmetric cell division is a key step in cellular differentiation in multicellular organisms. In plants, asymmetric zygotic division produces the apical and basal cells. The mitogen-activated protein kinase (MPK) cascade in *Arabidopsis* acts in asymmetric divisions such as zygotic division and stomatal development, but whether the effect on cellular differentiation of this cascade is direct or indirect following asymmetric division is not clear. Here, we report the analysis of a rice mutant, *globular embryo 4 (gle4)*. In two- and four-cell-stage embryos, asymmetric zygotic division and subsequent cell division patterns were indistinguishable between the wild type and *gle4* mutants. However, marker gene expression and transcriptome analyses showed that specification of the basal region was compromised in *gle4*. We found that *GLE4* encodes MPK6 and that *GLE4/MPK6* is essential in cellular differentiation rather than in asymmetric zygotic division. Our findings provide a new insight into the role of MPK in plant development. We propose that the regulation of asymmetric zygotic division is separate from the regulation of cellular differentiation that leads to apical-basal polarity.

KEY WORDS: Rice, GLOBULAR EMBRYO 4, GLE4, MPK6, Embryogenesis

INTRODUCTION

The formation of body axes, such as the apical-basal axis, is a key step in early embryogenesis in multicellular organisms. The shoot and root apical meristems in flowering plants are formed according

to the positional information based on the apical-basal axis (Jürgens, 2001). In *Arabidopsis thaliana*, mutations affecting apical-basal axis formation often result in severe defects in embryogenesis (Mayer et al., 1991).

The zygote divides asymmetrically, producing a small apical cell with a dense cytosol and a large basal cell with well-developed vacuoles in *Arabidopsis* (Jürgens, 2001). The apical cell generates the pro-embryo, and the basal cell divides to produce the extra-embryonic suspensor and hypophysis. Mutations affecting asymmetric zygotic cell division affect specification of the basal or apical region (Bayer et al., 2009; Jeong et al., 2011; Lukowitz et al., 2004; Yu et al., 2016). This division is regulated by a mitogen-activated protein kinase (MPK) cascade that includes YODA (YDA) MPK kinase (MPKKK) in *Arabidopsis* embryo (Lukowitz et al., 2004). The loss-of-function *yda* mutants lack basal cell identity and the suspensor, whereas constitutively active YDA exaggerates suspensor development. YDA also regulates asymmetric cell division in stomatal development (Bergmann et al., 2004). MPK3 and MPK6 function downstream of YDA (Wang et al., 2007). Similar to the *yda* mutant, the loss-of-function *mpk3 mpk6* double mutant undergoes zygotic cell division with two similar daughter cells and loses the basal domain (Wang et al., 2007). It has also been shown that MPK6 and its upstream MKK4/5 in *Arabidopsis* are involved in embryo development (Bush and Krysan, 2007; López-Bucio et al., 2014; Zhang et al., 2017). The YDA-MPK3/6 pathway is activated by the interleukin 1 receptor-associated kinase (IRAK)/Pelle-like kinase gene *SHORT SUSPENSOR (SSP)* transcribed in sperm cells and by the peptide named EMBRYO SURROUNDING FACTOR 1 (ESF1), which accumulates in the central cell before fertilization (Bayer et al., 2009; Costa et al., 2014). Thus, the YDA-MAPK3/6 pathway, which is activated by stimuli from the parental origin regulates asymmetric cell division and results in the specification of the basal region. Thus, in *Arabidopsis*, asymmetric zygotic division is directly linked to apical-basal patterning.

WUSCHEL-RELATED HOMEBOX (WOX) transcription factors are early markers for the apical or basal cell fate in *Arabidopsis*. The expression of WOX8 and WOX9 is regulated by WRKY2, the activity of which is regulated by YDA pathway-mediated phosphorylation in the basal cell and specifies its fate (Haecker et al., 2004; Ueda et al., 2011, 2017). WOX8 and WOX9 also non-autonomously promote the expression of WOX2 in the apical cell (Breuninger et al., 2008; Haecker et al., 2004).

In monocots, the mechanism of polarity establishment and organogenesis in early embryogenesis is less studied than in *Arabidopsis*, but orthologues of many genes involved in early embryogenesis in *Arabidopsis* are found in monocots (Itoh et al., 2016; Zhao et al., 2017). The expression of *ZmWOX9A* and

¹Department of Plant Production Sciences, Graduate School of Bioagricultural sciences, Nagoya University, Nagoya, Aichi 464-8601, Japan. ²Molecular Genetics Department, National Institute of Agrobiological Sciences, 2-1-2 Kannondai, Tsukuba, Ibaraki 305-8602, Japan. ³Department of Agricultural and Environmental Biology, Graduate School of Agricultural and Life Sciences, University of Tokyo, Tokyo 113-8657, Japan. ⁴Genome Resource Unit, Agrogenomics Resource Center, National Institute of Agrobiological Sciences, 2-1-2 Kannondai, Tsukuba, Ibaraki 305-8602, Japan. ⁵National Institute of Genetics, 1111 Yata, Mishima, Shizuoka 411-8540, Japan. ⁶College of Bioscience and Biotechnology, Chubu University, Kasugai, Aichi 487-8501, Japan.

*Present address: Aichi Agricultural Research Center, Nagakutecho, Aichi 480-1103, Japan. †Present address: Institute of Vegetable and Floriculture Science, National Agriculture and Food Research Organization, 2-1 Fujimoto, Tsukuba, Ibaraki 305-0852, Japan. ‡Present address: School of Agricultural Regional Vitalization, Kibi International University, Minamiawaji, Hyogo 656-0484 Japan. ¶Present address: Institute of Crop Science, National Agriculture and Food Research Organization, 2-1-2 Kannondai, Tsukuba, Ibaraki 305-8518, Japan. **Present address: Aishin Cosmos R&D Co., Ltd., 2-36 Hachiken-cho, Kariya, Aichi 448-8650, Japan. ††Present address: Biotherapy Institute of Japan, 1-18-2 Sakura, Tsukuba, Ibaraki 305-0003, Japan.

§§Author for correspondence (yusato@nig.ac.jp)

© K.-i.H., 0000-0001-8578-7276; Y.S. (NIG), 0000-0002-0751-6611; T.S., 0000-0002-1977-0510

ZmWOX9B, which are *WOX8* and *WOX9* counterparts in maize, is detectable shortly after fertilization, but that of *ZmWOX2*, an orthologue of *Arabidopsis WOX2*, is detected much later in maize embryogenesis (Chen et al., 2017; Nardmann et al., 2007). Thus, the involvement of *WOX* genes in apical and basal patterning is not the same in *Arabidopsis* and maize.

In this study, we have analyzed the *globular embryo 4 (gle4)* rice mutant and propose a model for apical-basal patterning in early embryogenesis in rice. This mutant produces a round-shaped embryo without organ differentiation (Hong et al., 1995; Kamiya et al., 2003). We found that *GLE4* encodes OsMPK6, the *Arabidopsis* orthologue of which regulates asymmetric cell divisions in the zygote and meristemoid mother cell (Wang et al., 2007). Three groups have reported mutations in this gene in rice (Liu et al., 2016; Minkenberg et al., 2017; Yi et al., 2016); however, these studies did not analyze asymmetric zygotic division or apical-basal patterning.

We examined the phenotypes of *gle4/osmpk6* with a focus on zygotic asymmetric division and apical-basal patterning. We found that *GLE4/OsMPK6* is essential for cellular differentiation rather than for asymmetric zygotic division and determines the basal region at the early stage of rice embryogenesis. Our findings provide a new insight into cellular differentiation and asymmetric division through the function of MPK signaling, and raise the possibility that the asymmetric zygotic division and cellular differentiation that lead to apical-basal polarity can be separately regulated.

RESULTS

The globular shaped embryo 4 (*gle4*) mutant has defective organogenesis

The original *gle4* lines, *gle4-1* and *gle4-2*, were described as globular shaped embryo mutants and were isolated from a collection of organogenesis-defective mutant rice stock (Hong et al., 1995); the other three *gle4* lines, *gle4-3*, *gle4-4* and *gle4-5*, were obtained by screening mutants with a similar phenotype to *gle4* from chemical- and transposon-induced mutant populations. All five lines showed segregation of mutant embryos in a manner of single recessive inheritance (Table S1). All five lines are heterozygotes and we have never recovered homozygous plants, suggesting embryo lethality of these mutations. The embryo phenotype in all five mutant alleles is stable and similar (Fig. S1). The *gle4* embryos were globular, but were not globular arrested, because they grew beyond the globular stage while keeping the shape globular (Fig. 1B,C). Until 3 days

after pollination (DAP), the *gle4* embryos were morphologically indistinguishable from wild-type embryos (data not shown, see Fig. 3 upper and lower panels). At 4 to 6 DAP, wild-type embryos started to form the coleoptile, shoot apical meristem and root apical meristem (Fig. 1D-F), whereas *gle4* failed to form discrete organs or tissues except for epithelium-like epidermis and a mass of small cells that resembled vascular tissues at the center (Fig. 1G-I). This is consistent with a previous report showing the expression of several protodermal genes such as *ROC1* and *RAmy1A*, and a vasculature-specific gene, *OsPNH*, in *gle4* (Kamiya et al., 2003). The morphological phenotypes are similar to previously reported *osmpk6* mutants in rice, although the expression pattern of protodermal genes is different (Yi et al., 2016; see later). At 9 DAP, organogenesis in wild-type embryos was completed, but most of the organs were missing in *gle4* embryos (Fig. 1A-C).

In the wild type, the suspensor at the base of the embryo connects it with mother tissue (Fig. S2) and is composed of a population of round-shaped cells resembling a cluster of grapes; no such cell population was found at the base of mutant embryos (Fig. S2). Overall, the *gle4* mutant phenotype suggests that *GLE4* regulates organogenesis during embryogenesis.

Molecular cloning of *GLE4*

We cloned *GLE4* by transposon tagging using *gle4-3*, which was derived from a *TOS17* transposon mutagenesis library (Figs S3 and S4). We found that *GLE4* encoded OsMPK6 (locus ID Os06g0154500), a member of the MPK family and an orthologue of *Arabidopsis* MPK6. We conducted molecular complementation using *gle4-3* mutant homozygous calli. As described by Kamiya et al. (2003), it is possible to induce and culture *gle4* mutant homozygous calli on culture medium, although mutant calli do not regenerate normal shoots but produce many small leaf like organs on the regeneration medium (Kamiya et al., 2003). We used this character to assess molecular complementation. We infected *gle4-3* homozygous mutant calli with agrobacterium harboring the complementation vector carrying *OsMPK6* cDNA under the control of ubiquitous promoter, and placed on the regeneration medium to see whether the normal shoots regenerate from mutant calli. As shown in Fig. S5, the normal shoots and plants were regenerated and recovered from *gle4-3* mutant homozygous calli by the introduction of the complementation vector, whereas the introduction of kinase inactive mutant vector of OsMPK6 cDNAs did not regenerate normal shoots. Thus, molecular

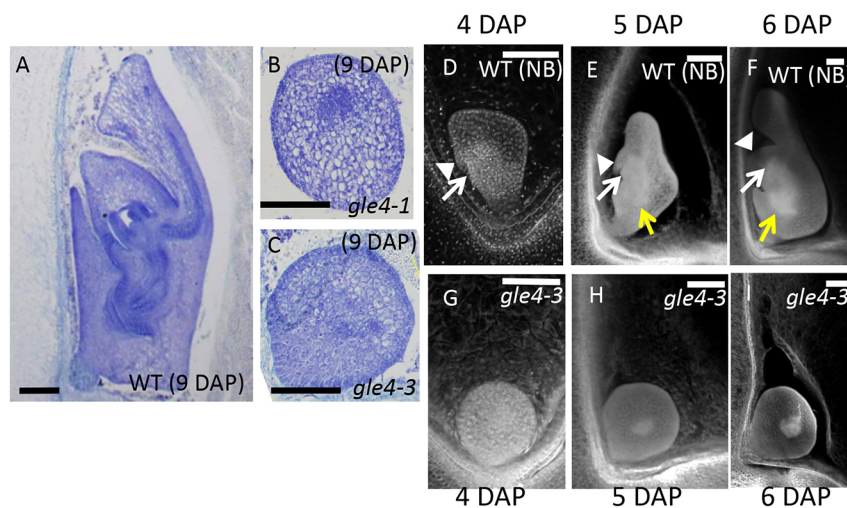


Fig. 1. Morphology of *gle4* embryos. (A-C) Longitudinal sections of embryos at 9 days after pollination (DAP) in wild type (WT) (A), *gle4-1* (B) and *gle4-3* (C). Scale bars: 50 μm. (D-I) Time course of embryo development in wild type (D-F) and *gle4-3* mutant (G-I). Embryos were stained with Toluidine Blue-O (A-C) or Propidium Iodide (D-I) and examined by light microscopy or confocal microscopy. Scale bars: 100 μm. White triangle, white and yellow arrows indicate coleoptile, shoot apical meristem and root apical meristem, respectively. NB, Nipponbare.

complementation analysis supported the cloning of *GLE4*. *gle4-2* and *gle4-3* carry a splice site mutation and *Tos17* transposon insertion, respectively, within the conserved kinase catalytic domain, and *gle4-4* and *gle4-5* carry nonsense mutations within the conserved kinase catalytic domain (Fig. S4). *gle4-1* carries missense mutation (G213E) in the conserved kinase catalytic domain. The glycine residue at 213 amino acid residue of OsMPK6 is highly conserved residue among MPK family in plants (Fig. S4). Based on the similarity of the phenotype and the mutant lesions of five alleles, we consider that those are all null alleles. This is consistent with previous reports, which showed that the loss-of-function mutations in *OsMPK6* result in similar embryo lethality (Yi et al., 2016; Minkenberg et al., 2017). Yi et al. (2016) reported two insertion alleles of *OsMPK6*, *osmpk6-1* and *osmpk6-2*. Although, they argue that there are some difference in the expression of epidermal marker genes such as *ROC1* or *RAmy1A* between *osmpk6* and *gle4* described by Kamiya et al. (2003), this could be merely due to the difference in the timing of embryo RNA sampling.

Patterns of cell division in *gle4* mutant embryos at early stages

Because the embryos of *Arabidopsis* MPK pathway mutants (such as *yda* or *mapk3 mapk6* double mutant) fail in the asymmetric

zygotic division and often have no discrete organs (Lukowitz et al., 2004; Wang et al., 2007), we investigated the cell division patterns of the rice zygote and early embryo of the wild type and *gle4*.

Fig. S6 shows the course wild-type embryogenesis in rice at early stages. In the wild-type embryos, zygotes divided into small apical and large basal cells (Fig. 2A), although the elongation of the zygote was not as evident as in *Arabidopsis* (Lukowitz et al., 2004). Apical and basal cells divided to form the four-cell stage embryo (Fig. 2B). The angle between the planes of this second round of cell division appeared to be random (Fig. 2E), which result in various arrangements of the four embryonic cells. The cell divisions therefore seem to occur unpredictably, which is commonly observed in monocots and dicots, although not in *Arabidopsis* (Wardlow, 1955).

To compare the pattern of zygotic and early embryo cell divisions in *gle4* mutants, we analyzed *gle4* segregating ovaries by self-pollination of heterozygous *gle4* plants; we expected to recover approximately 25% of mutant embryos (Table S1). In *gle4* segregating ovaries, all of the 17 two-cell embryos showed smaller apical and larger basal cells similar to those of the wild type, suggesting no obvious differences in zygotic division between the wild type and *gle4* (Fig. 2C,D). In all of the 35 *gle4* segregating ovaries, the four-cell-stage embryos had a small apical side and large basal side; the cellular arrangement was indistinguishable

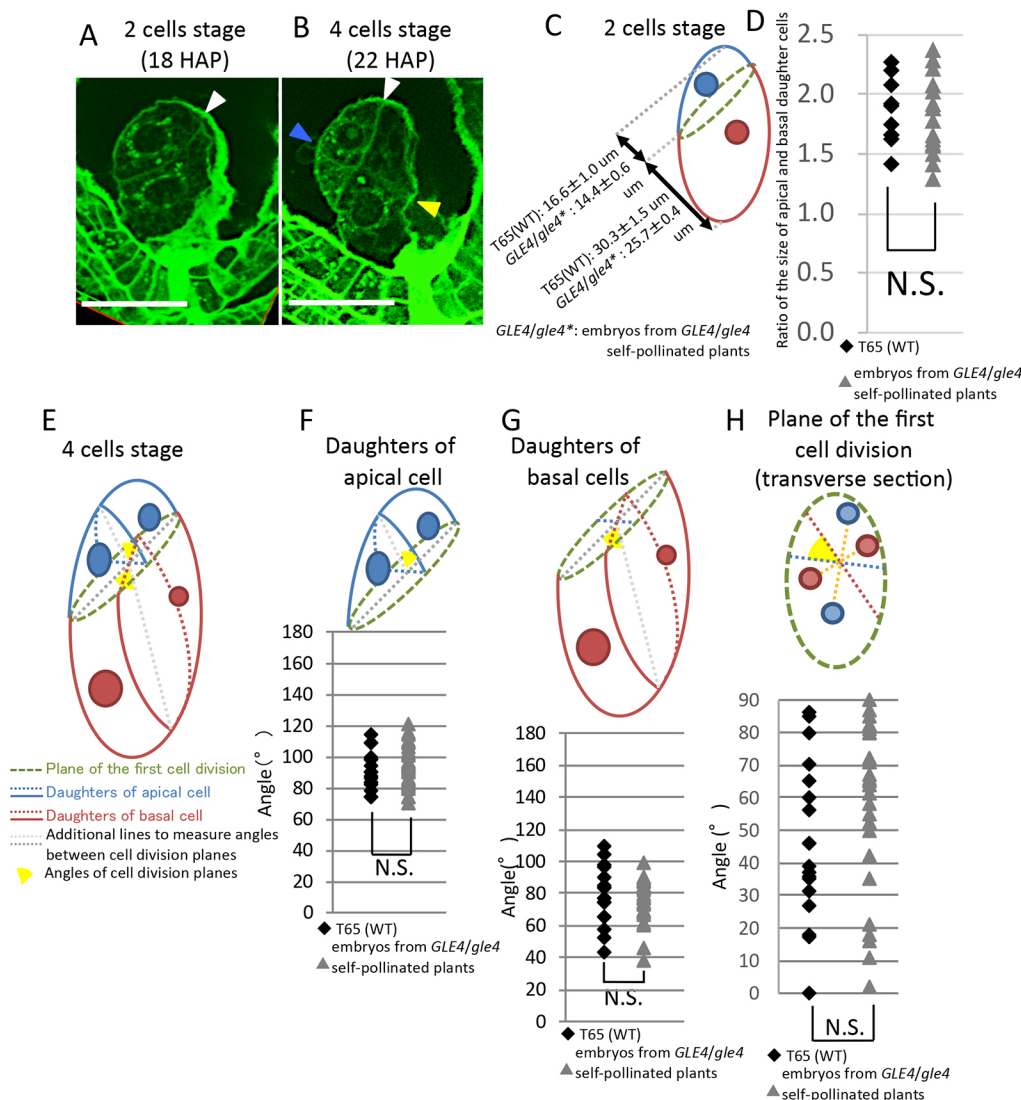


Fig. 2. Cell division pattern in early *gle4* embryos.

(A) Two- and (B) four-cell embryos from the *GLE4/gle4* self-pollinated plants. Scale bars: 30 μ m. Positions of cell division planes: first, white triangles; apical, blue triangle; basal, yellow triangle. (C) A scheme showing a two-cell stage embryo and the length of the apical and basal daughter cells of the zygote in embryos from wild type and from the *GLE4/gle4* self-pollinated plants (data are mean \pm s.e.m.); $n=10$ and 17 for wild-type embryos and embryos from the *GLE4/gle4* self-pollinated plants, respectively. *GLE4/gle4**, embryos from the *GLE4/gle4* self-pollinated plants. (D) Ratio of the size of apical and basal daughter cells of the zygote. Wild type, $n=10$; *GLE4/gle4**, $n=17$. N.S., not significant by the *F*-test in ANOVA; $P=0.92$. (E) A scheme showing a four-cell stage embryo. (F-H) Angles between cell division planes in four-cell stage embryos from T65 (wild type) and from *GLE4/gle4* self-pollinated plants. (F) Apical cell division versus the first cell division. (G) Basal cell division versus the first cell division. (H) Apical versus basal cell divisions. The scheme in H represents a transverse section image around the plane of the first division. This is different from the schemes in F and G. All embryos were stained using the pseudo-Schiff method. Wild type, $n=30$; *GLE4/gle4*, $n=35$. N.S., not significant by the *F*-test in ANOVA; $P=0.63$ in F, $P=0.14$ in G, H. HAP, hours after pollination.

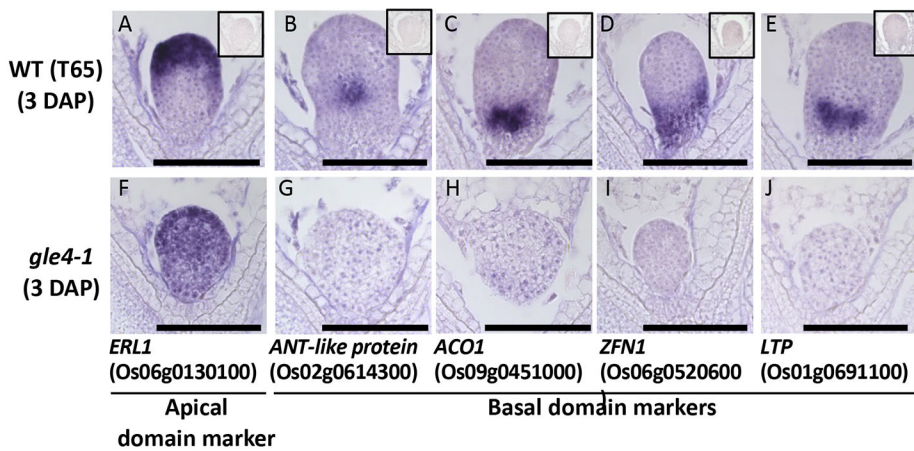


Fig. 3. *In situ* hybridization with probes for five embryo domain-specific marker genes in 3 DAP wild-type and *gle4-1* embryos. (A, F) Apical marker gene *ERECTA like kinase 1* (*ERL1*) in wild type (A) and *gle4-1* (F). (B-E, G-J) Basal region-specific marker genes: *ANT-like protein* in wild type (B) and *gle4-1* (G); *ACC oxidase 1* (*ACO1*) in wild type (C) and *gle4-1* (H); *Zinc finger nuclease 1* (*ZFN1*) in wild type (D) and *gle4-1* (I); and *Lipid transfer protein* (*LTP*) in wild type (E) and *gle4-1* (J). Insets in the upper right corners are the control sense-probe hybridizations. Scale bars: 100 μ m.

between *gle4* and the wild type (Fig. 2B, F-H). To confirm the latter observation, we assessed the cell arrangement by mapping the positions of the nuclei (Fig. 2F-H). By setting virtual planes between the nuclei of the two daughter cells of the apical or basal cells, we measured the angles of the intersections of the two planes, compared their distributions between the wild type and the mutant segregating population (Fig. S7), and found no difference (Fig. 2F-H). This suggests that *OsMPK6* is dispensable for cell division patterning at an early stage of embryogenesis in rice.

Regional differentiation in *gle4* mutant embryos

Asymmetric zygotic division in both the wild-type and *gle4* embryos suggested that apical-basal polarity was normal in the mutant embryos. To confirm this, we tested marker gene expression in the wild type and mutant segregating populations. We have previously developed a set of marker genes that indicate regional differentiation at early stages of rice embryogenesis (Itoh et al., 2016). We used one apical marker and four basal markers for *in situ* hybridization analysis at 3 DAP. Unexpectedly, the apical marker was expressed in the entire *gle4* embryo, whereas the expression of basal marker genes was mostly abolished (Fig. 3). Thus, in the *gle4* embryo, the identity of the basal region is lost, and the cells acquire apical character.

We further confirmed this by transcriptome analysis of RNA recovered by laser microdissection (LMD) from 3 DAP embryo of wild type and *gle4-1*. Briefly, we extracted total RNA from embryos recovered by LMD then genotyped each embryo by DNA sequencing after cDNA synthesis, because, at 3 DAP there is no morphological difference and we could not distinguish wild-type and *gle4-1* embryos. Mixtures of RNA from three mutant or wild-type embryos were then subjected to transcriptome analysis with triplicates for both (Fig. S8). A summary of RNA-sequencing experiment is shown in Table S2. We detected expression of 20,737 and 20,834 genes in wild-type and mutant embryo, respectively. Among them, 725 genes and 604 genes were differentially expressed in *gle4-1* at high and low levels, respectively at $FDR < 0.001$ (Figs S9 and S10). A list of differentially expressed genes is shown in Tables S3 and S4. We compared these differentially expressed genes (DEGs) with the list of genes with localized expression in 3 DAP embryo at the apical and basal sides that were identified in our previous work (Itoh et al., 2016) (Fig. 4A-C). We discovered that the majority of genes with low expression in *gle4-1* were genes expressed at the basal side in wild type (Fig. 4A, B), and those with high expression in *gle4-1* were genes expressed at apical side in the wild type (Fig. 4A, C). The transcriptome analysis

also suggests that, in the *gle4* embryo, the identity of the basal region is lost and the cells acquire apical character.

Next, we compared DEGs with the list of genes expressed at shoot, scutellum, epiblast and radicle at 7 DAP of wild type (Itoh et al., 2016) (Fig. 4D-F). The majority of genes with high expression in *gle4-1* were scutellum-specific genes at 7 DAP. This suggests

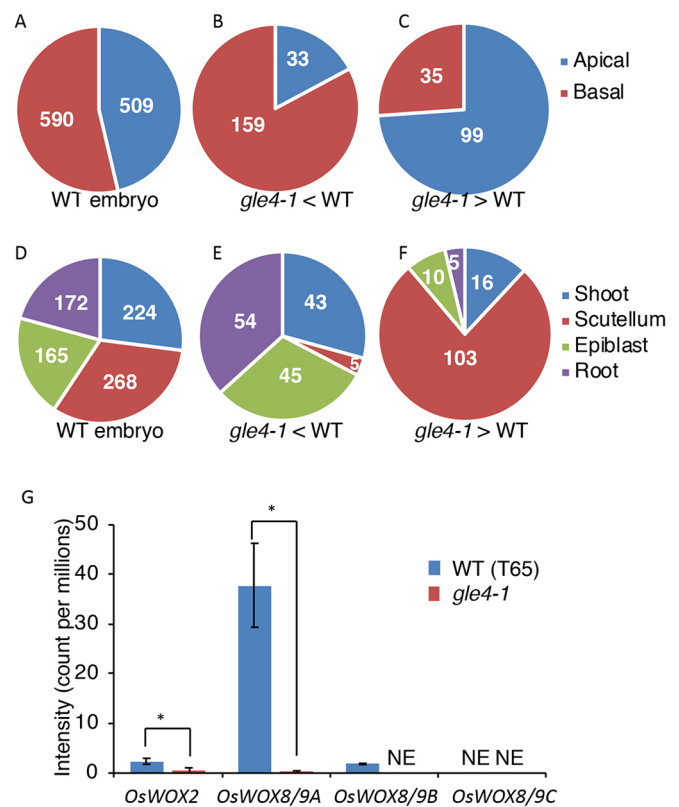


Fig. 4. Transcriptome analysis of 3 DAP embryo recovered by laser microdissection from wild type and *gle4-1*. (A-C) Number of genes expressed at apical or basal regions in 3 DAP embryo reported by Itoh et al. (2016) in wild-type samples (A), in DEG with reduced expression in *gle4-1* (B) and with elevated expression in *gle4-1* (C). (D-F) Number of genes with tissue-specific expression at 7 DAP in wild type (D), in DEG with reduced expression in *gle4-1* (E) and in DEG with elevated expression in *gle4-1* (F). (G) Expression of WUSHCEL-related homeobox (WOX) genes (*OsWOX2*, Os01g0840300; *OsWOX8/9A*, Os01g0667400; *OsWOX8/9B*, Os05g0118700; *OsWOX8/9C*, Os07g0533201) in 3 DAP wild-type and *gle4-1* embryos. * $P < 0.05$. NE, not expressed.

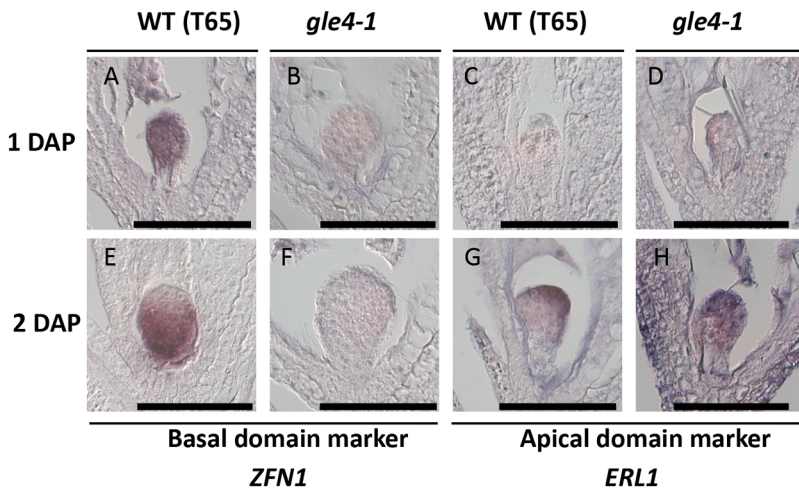


Fig. 5. *In situ* hybridization with probes for two embryo domain-specific marker genes in 1 and 2 DAP wild-type and *gle4-1* embryos. (A-D) The basal marker gene *Zinc finger nuclease (ZFN1)* in wild type (A) and *gle4* (B), and the apical marker gene *ERECTA like kinase 1 (ERL)* in wild type (C) and *gle4* (D). (E-H) *ZFN1* in wild type (E) and *gle4* (F), and *ERL* in wild type (G) and *gle4* (H). Scale bars: 100 μ m.

that, at 3 DAP in the wild type, the apical side is destined to become scutellum and the basal side mainly constitutes the remaining parts such as shoot, epiblast and radicle. We further investigated the expression of rice *OsWOX2* and *OsWOX8/9*, whose *Arabidopsis* orthologues are expressed in apical (*WOX2*) and basal (*WOX8/9*) cells (Zhang et al., 2010). In the transcriptome data, *OsWOX2*, *OsWOX8/9A* and *OsWOX8/9B* expression was detected in the wild type and the expression levels of both genes were decreased or not detected in *gle4-1*, although the expression level of *OsWOX2* and *OsWOX8/9B* are very low in the wild type at this stage (Fig. 4G). Because *WOX8/9* expression in *Arabidopsis* resides in the basal region, the reduction of *OsWOX8/9* in *gle4-1* is expected. Interestingly, *OsWOX2* expression is also decreased in *gle4-1*. Thus, the expression pattern of *OsWOX2* at early embryogenesis is not the same as *WOX2* in *Arabidopsis*.

To test whether *OsMPK6* is involved in the establishment and/or maintenance of basal region identity, we examined the expression of one apical and one basal marker at 1 and 2 DAP. In the wild type, the basal marker was expressed in the entire embryo at 1 DAP (Fig. 5A) and its expression became localized at the embryo base at 2 DAP (Fig. 5E); the apical marker was undetectable at 1 DAP but started to be expressed at 2 DAP (Fig. 5C,G). In *gle4* segregating embryos, the expression of the apical marker was not detected at 1 DAP (Fig. 5D), but it appeared in the entire embryo at 2 DAP (Fig. 5H); the basal marker was not detected at 1 or 2 DAP (Fig. 5B,F). Overall, these data indicate that the entire rice embryo has basal identity at 1 DAP, the apical region is established at 2 DAP and *GLE4/MPK6* is indispensable for the establishment and/or maintenance of the basal region (Fig. 6).

DISCUSSION

The molecular genetic analysis of the model plant *A. thaliana* has deepened our knowledge of the embryogenesis of flowering plants. The simple and stereotyped pattern of cell divisions in *Arabidopsis* embryos at early stages facilitates the tracing and prediction of cell divisions until a fairly late stage (e.g. heart stage). Most textbooks introduce the *Arabidopsis* embryo as a model for embryogenesis in flowering plants, but many flowering plants undergo embryogenesis with more unpredictable cell divisions after zygotic division (Wardlaw, 1955). The stereotyped cell divisions imply that cellular lineage is important for regional differentiation in embryogenesis, but the basic body pattern of the plant embryo is maintained even in mutants with disturbed cell division patterns in early embryogenesis (Torres-Ruiz and Jürgens, 1994; Spinner et al.,

2013). This suggests that regional differentiation in the embryo does not depend on cellular lineage information.

Using rice *gle4* mutants, we showed that *GLE4* encodes *OsMPK6*, an orthologue of *Arabidopsis* *MPK6* and that *gle4* mutants undergo asymmetric zygotic division similar to that of the wild type. We also found that the *osmpk3 gle4/ osmpk6* double mutant rice embryo is indistinguishable from that of the *gle4/osmpk6* single mutant (Fig. S11). In addition, our previous analysis of gene expression profiles in early stages of rice embryogenesis revealed that *OsMPK3* expression is very low (Itoh et al., 2016; RICEXPRO database, ricexpro.dna.affrc.go.jp).

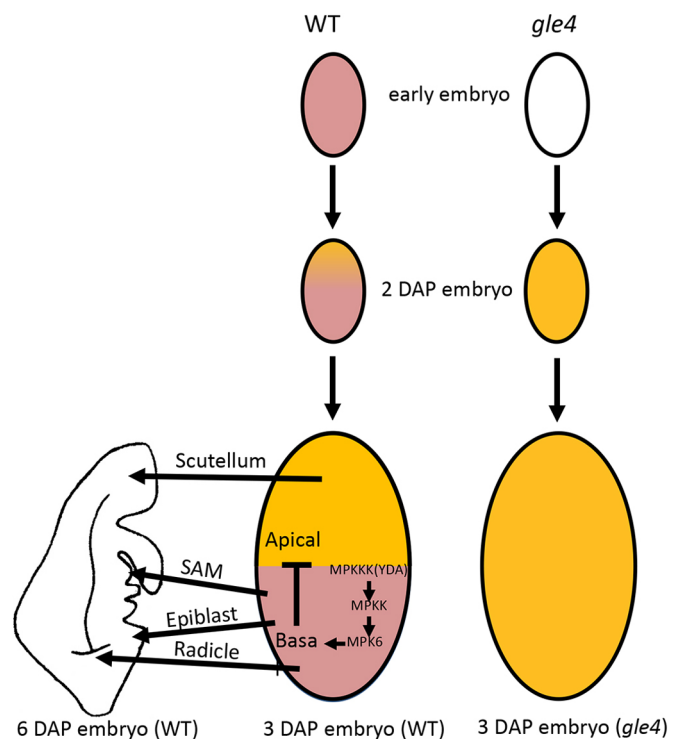


Fig. 6. Role of the MPK cascade that includes *MPK6* in apical-basal patterning during early embryogenesis in rice. In wild type, the cascade directs basal cell identity during early embryogenesis and we hypothesize that the basal region prevents over-proliferation of the apical region. In *gle4* embryos, the basal region is replaced with the apical region with the character of scutellum, resulting in the absence of most organs, including shoot apical meristem.

These suggest that the MPK cascade that includes OsMPK3 and OsMPK6 is dispensable for asymmetric zygotic division in rice.

In zygotic division in rice, small apical and large basal cells are formed (Fig. 2A,C,D); the cells then divide to form a four-cell embryo. We showed that the arrangement of the daughter cells of the apical and basal cells is arbitrary both in the wild type and *gle4*. This is consistent with the observations that many monocot and dicot species undergo non-stereotyped cell divisions after asymmetric zygotic division (Wardlow, 1955). Because the first sign of morphological abnormality in *gle4* is observed in the 4 DAP embryo, which consists of more than 1000 cells, we speculate that GLE4 acts in regional specification at earlier stages and/or it functions in organogenesis. Using a set of region-specific markers in the early rice embryo, we showed that GLE4 is pivotal for the establishment or maintenance of the basal region, which occurs by 1 DAP (Figs 3-5).

Mutations in the *Arabidopsis* YDA (MPKKK)-MPK3/6 cascade lead to a defect in asymmetric zygotic division and result in two daughter cells of similar size (Lukowitz et al., 2004). This is similar to the *gle4* phenotype because in both cases the basal part is absent, suggesting that the fundamental function of the MPK3/6 pathway in early embryogenesis is the establishment and/or maintenance of the basal region. In *Arabidopsis*, the establishment/maintenance of the basal region directed by the MPK3/6 pathway occurs at the asymmetric zygotic division, whereas in rice it occurs after this division. In rice, asymmetric zygotic division and MPK3/6-dependent basal specification can be uncoupled and are controlled by different systems. We cannot exclude the possibility that yet unknown genes are involved specifically in the apical or basal cell specification after zygotic division both in the wild type and *gle4*, i.e. the presence of another layer of apical-basal polarity establishment independent of the MPK3/6 pathway.

Analysis using our marker gene sets suggested that, in early rice embryo, the basal identity may appear first by all cells by 1 DAP, and then the apical marker starts to be expressed. The transcriptome analysis of 3 DAP embryo also revealed that the apical region mainly contributes to the scutellum and the rest of the embryonic organs such as the shoot, epiblast and radicle are from the basal region. This is the reason why *OsWOX2* and many other SAM-specific genes, such as *OSH1*, were downregulated in *gle4* (Fig. 4G) (Kamiya et al., 2003; Sato et al., 1996). Interestingly, the loss of basal identity in *gle4* leads to expansion of apical character in mutant embryo, suggesting there is a competitive regulation and interaction between apical and basal regions (Fig. 6). Similar interactions between embryonic domains have been reported in *Arabidopsis* (Breuninger et al., 2008; Smith and Long, 2010). Even though the origin of the shoot apical meristem is different between rice and *Arabidopsis*, the interaction between apical and basal regions seems conserved.

In the asymmetric zygotic division in *Arabidopsis*, the YDA-MPK3/6 cascade is activated by a paternal gene product named Short Suspensor (SSP), a cytoplasmic receptor kinase (Bayer, et al., 2009). In the asymmetric division of meristemoid mother cells, this MPK pathway regulates BASL, which shows polarized localization in cells (Dong et al., 2009). No clear orthologue of SSP or BASL is encoded in the rice genome, suggesting that, although this MPK pathway, including MPK3/6, is conserved, its input and output have diverged among flowering plants. This is consistent with the fact that MPK3/6 signaling is activated by changing biotic stresses such as pathogen infections. The signals upstream and downstream of the rice GLE4/OsMPK6 pathway involved in regional specification in the early rice embryo remain to be elucidated.

MATERIALS AND METHODS

Plant materials and growth conditions

The *gle4-1*, *gle4-2*, *gle4-4* and *gle4-5* seeds were obtained from chemically mutagenized populations, and *gle4-3* seeds were from a *Tos17*-mutagenized population (*gle4-3*). To observe cell division patterns at 18 and 24 h after pollination (HAP), *gle4-1*^{+/-} and Taichung 65 seedlings were grown in a controlled growth chamber as described by Ohnishi et al. (2011). To obtain samples for *in situ* hybridization and histological observations of 4-9 DAP embryos, *gle4-1*^{+/-} and *gle4-3*^{+/-} seedlings were grown in a paddy field.

Transposon tagging

The heterozygous lines of *gle4-3* were grown in paddy field and 2-3 g of leaves were harvested from each plant for genomic DNA extraction (Agrawal et al., 2001). We harvested seeds from each plant after self-pollination, and determined the genotype of each plant by counting the segregation of mutant embryo as wild type (WT) or heterozygous (H). Based on this genotype, we used the linkage with the *TOS17* insertion described by Agrawal et al. (2001). The flanking sequence of *TOS17* insertion was recovered using a thermal asymmetric interlaced PCR method followed by DNA sequencing (Miyao et al., 2003).

Production of transgenic plants

For molecular complementation test, a 1.7 kb cDNA encoding OsMPK6 (Os06g0154500) was inserted downstream of the 35S promoter in the binary vector pB1101-Hm. The procedure to introduce the kinase inactivation mutations to OsMPK6 is described in Kishi-Kaboshi et al. (2010). The resulting plasmid was introduced into *Agrobacterium tumefaciens* EHA101, which was then used to transform mutant calli as described by Hiei et al. (1994).

Phenotypic observation of *gle4* embryos

Pistils containing embryos at 4-9 DAP were cut in half and fixed in 37% formaldehyde:glacial acetic acid:70% ethanol (1:1:18) under vacuum three times for 15 min each and then overnight. Fixed embryos were hydrated through a graded ethanol series with a microwave processor (250 W, 1.5 min each step) on ice. Solution was replaced with 1×PBS, and the embryos were stained with 50 µg/ml propidium iodide containing 100 µg/ml RNase in 1×PBS overnight in the dark at 37°C. Embryos were dehydrated through an ethanol series and cleared by methyl salicylate with a microwave processor (300 W, 1.5 min each step) on ice. Propidium iodide fluorescence emission at 570-670 nm (excitation at 559 nm) was captured using confocal microscopes (FV1000 and FV3000; Olympus).

To prepare samples for scanning electron microscopy, 7 DAP embryos were fixed in 4% paraformaldehyde and 0.25% glutaraldehyde in 0.05 M sodium phosphate buffer (pH 7.2) under vacuum at room temperature for 1 h and then overnight. The samples were dehydrated through a graded ethanol series and t-butanol series, and t-butanol was sublimated under vacuum at a sub-zero temperature. Samples were coated with platinum ion and observed under a scanning electron microscope (S-3000N; Hitachi).

To observe cell division patterns during early embryogenesis, ovules in pistils isolated at 18 and 24 HAP were stained by the pseudo-Schiff method (Vollbrecht and Hake, 1995). Acriflavine fluorescence emission at 530-630 nm (excitation a 515 nm) was captured using the FV1000 microscope.

Construction of a 3D model of nucleus position

Using coordinates of the nuclei in confocal images of embryos at the two- or four-cell stage, we plotted nucleus positions and constructed a 3D model (see Fig. S7). At the two-cell stage, the nuclei of the apical and basal cells were connected with a line. The distance from the top of the apical cell or the bottom of basal cell to the plane perpendicular to this line was measured. For the four-cell stage, nuclei of each apical and each basal cell were connected by lines (A_{apical} and A_{basal}). Planes perpendicular to these lines were named plane 1 and plane 2, respectively. Plane 3 was perpendicular to line B, which connected the midpoints of the A_{apical} and A_{basal} lines. The angles between planes 1 and 3, and planes 2 and 3, and between the intersections of planes 1 and 3 (line C) and planes 2 and 3 (line D) were measured and are presented in Fig. 2F-H, respectively. The 3D-model construction and the

measurements were performed using a FV10-ASW 4.2 viewer (Olympus) and Metasequoia (Tetraface) software.

In situ hybridization

Sections (8 μ m) were cut with a rotary microtome. *In situ* hybridization was performed as described previously (Kouchi and Hata, 1993). To produce DIG-labeled *OsMPK6* sense and antisense probes, a 900 bp DNA fragment was amplified by PCR from a cDNA clone provided by NIAS Japan (AK111942) and used as a template for *in vitro* transcription with a Maxi Script *in vitro* transcription kit (Thermo Fisher Scientific). Probes for transcripts specific for the apical or basal region were prepared as described previously (Itoh et al., 2016). Hybridization was conducted at 52°C overnight.

Laser microdissection (LMD)

Ovaries of *gle4-1* heterozygous plants at 3 DAP were fixed in 75% ethanol:25% acetic acid. After dehydration in a graded ethanol series, the tissues were embedded in paraffin and sectioned at 16 μ m. Complete serial sections of embryo regions were placed onto PEN membrane glass slides (Leica) as described previously (Takahashi et al., 2010). After drying at 42°C, slides were immersed in 100% HistoClear II (National Diagnostics) for 10 min twice to remove paraffin, followed by air-drying at 4°C. Three or four sections covering the entire one embryo were collected into a tube from sections using a Leica LMD6000 Laser Microdissection system.

RNA extraction from LMD samples

Total RNAs were extracted from the LMD-isolated tissues using a PicoPure RNA isolation kit (Life Technologies) according to the manufacturer's instructions. The qualities and concentrations of RNAs were measured using a 2100 Bioanalyzer (Agilent Technologies) with RNA6000 Pico kit (Agilent Technologies).

Genotyping of embryos recovered by LMD

After dissection of 131 embryos and extraction of RNAs, we genotyped each embryo as follows. From the embryo RNAs, cDNAs were synthesized using One Step SYBR PrimeScript RT-PCR Kit II (TAKARA) and then subjected to PCR amplification and DNA sequencing using primers (F4: GATACTGATCTGCATCAAATTA, R1: CAGCCACAGACCACATC) that amplify around the region of the *gle4-1* mutation site to determine the genotype of each embryo.

Transcriptome analysis of embryos recovered by LMD

Based on the results of genotyping mentioned above and RNA quality check, three mutants and three wild-type embryo RNAs with higher RNA quality were mixed into a single tube in triplicate. Thus, we prepared three wild-type and *gle4-1* samples using nine embryos for each. These RNA samples were converted to cDNA using the SMARTer Ultra Low Input RNA Kit for Sequencing-v4 (Clontech) according to the manufacturer's instructions. After converting cDNA, sequencing libraries were constructed using Nextera XT DNA Library Preparation Kit (Illumina). Sequencing was carried out with the Illumina HiSeq 2500 platform and the resulting reads were mapped to the reference genome of *Oryza sativa* (IRGSP 1.0) using RAP-DB annotations with STAR (Dobin et al., 2013). The 'quantMode' argument of STAR was used for reads counting. Transcript expression was evaluated using the EdgeR package in R (Robinson et al., 2010), and transcript abundance was estimated by counts per million mapped fragments (CPM). Differentially expressed genes were selected using FDR with $P < 0.001$ and fold change (FC) > 2 .

OsMPK3 (Os03g0285800) CRISPR/Cas9 vector construction

A method from Mikami et al. (2015) was used. The target sequence of *OsMPK3* was selected as 5'-AGCTTACGTTCTCGTGGTTCG-3' (antisense strand) by CRISPR-P v1.0 (cbi.hzau.edu.cn/cgi-bin/CRISPR). Selection criteria were as follows: (i) cleavage site in an exon; (ii) aggregate scoring for all possible gRNAs (guide RNAs) $S_{\text{guide}} > 95$; and (iii) close to the translation start site.

Production and observation of an *osmpk3* single mutant and an *osmpk3 osmpk6* double mutant

Seeds of a heterozygous plant with the *o-45* allele [*OsMPK6* (+/-)] were used for callus induction as in (Toki et al., 2016). Several calli were genotyped on the basis of the EcoRV digestion pattern of PCR products amplified with the following dCAPS primers: *o-45_F*, 5'-GCCACATGG-ACCACGAGGAT-3'; *o-45_R*, 5'-CAAAATCTGCCTAAAAATCGAG-3'. PCR was conducted following the manufacturer's instructions using GoTaq Colorless Master Mix (Promega). As homozygous *OsMPK6* (-/-) calli were not obtained, heterozygous *OsMPK6* (+/-) calli were used to generate transgenic plants. To create an *osmpk3* single mutant and a *osmpk3 osmpk6* double mutant, *OsMPK6* (+/-) calli were transformed with the *OsMPK3* CRISPR vector as described previously (Hiei et al., 1994). Each T1 seed of *OsMPK3 CRISPR/OsMPK6* (+/-) T0 plants was divided into the embryo and endosperm. Endosperm genomic DNA was used for genotyping. The *OsMPK3* genotypes of the T1 seeds were determined by sequencing the PCR products with the following primer set: *MPK3_genotyping_F1*, 5'-AGCGTAGTGGTTGACTGGTTG-3'; *MPK3_genotyping_R1*, 5'-CACAGTTCACCTACCTGGCAG-3'. PCR was conducted following the manufacturer's instructions with GoTaq Green Master Mix (Promega). The *OsMPK6* genotypes of the T1 seeds were determined as above. After genotyping, embryos of the wild-type, *osmpk3* single mutant, *osmpk6* single mutant and *osmpk3 osmpk6* double mutant were stained with Propidium Iodide, cleared with methyl salicylate and observed under a confocal laser scanning microscope (FV1200; Olympus).

Acknowledgements

We thank Dr Masaki Endo for providing vectors for CRISPR/cas9 experiments.

Competing interests

The authors declare no competing or financial interests.

Author contributions

Conceptualization: J.-i.L., K.-i.H., Y.S. (NARO), M.N., Y.N., H.H., Y.S. (NIG); Formal analysis: K.I., Y.S. (NIG); Investigation: K.I., S.S., M.K.-K., J.-i.L., K.-i.H., Y.S. (NARO), T.W., K.A., A.M., M.N.-T., Toshiya Suzuki, N.K.T., S.S.-S., H.T., Y.S. (NIG); Resources: K.I., Y.S. (NIG); Data curation: K.I., N.K.T., Takamasa Suzuki, A.T.; Writing - original draft: K.I., M.K.-K., J.-i.L., K.-i.H., Y.S. (NARO), M.N., Y.S. (NIG); Visualization: K.I.

Funding

This work was supported by a Japan Society for the Promotion of Science KAKENHI Grant-in-Aid for Scientific Research on Innovative Areas (17H06471) to Y.S.

Data availability

Nucleotide sequence data reported have been deposited in the DDBJ Sequence Read Archive under the accession number DRX155838, DRX155839, DRX155840, DRX155841, DRX155842 and DRX155843.

Supplementary information

Supplementary information available online at <http://dev.biologists.org/lookup/doi/10.1242/dev.176305.supplemental>

References

- Agrawal, G. K., Yamazaki, M., Kobayashi, M., Hirochika, R., Miyao, A. and Hirochika, H. (2001). Screening of rice viviparous mutants generated by endogenous retrotransposon *Tos17* insertion. tagging of a zeaxanthin epoxidase gene and a novel OsTATC gene. *Plant Physiol.* **125**, 1248-1257. doi:10.1104/pp.125.3.1248
- Bayer, M., Nawy, T., Gigliome, C., Galli, M., Meinel, T. and Lukowitz, W. (2009). Paternal control of embryonic patterning in *Arabidopsis thaliana*. *Science* **323**, 1485-1488. doi:10.1126/science.1167784
- Bergmann, D. C., Lukowitz, W. and Somerville, C. R. (2004). Stomatal development and pattern controlled by a MAPKK kinase. *Science* **304**, 1494-1497. doi:10.1126/science.1096014
- Breuninger, H., Rikirsch, E., Hermann, M., Ueda, M. and Laux, T. (2008). Differential expression of *WOX* genes mediates apical-basal axis formation in the *Arabidopsis* embryo. *Dev. Cell* **14**, 867-876. doi:10.1016/j.devcel.2008.03.008
- Bush, M. S. and Krysan, J. P. (2007). Mutational evidence that the *Arabidopsis* MAP kinase MPK6 is involved in anther, inflorescence, and embryo development. *J. Ex. Bot.* **58**, 2181-2191. doi:10.1093/jxb/erm092

- Chen, J., Strieder, N., Krohn, N. G., Cyprys, P., Sprunck, S., Engelmann, J. C. and Dresselhaus, T. (2017). Zygotic genome activation occurs shortly after fertilization in maize. *Plant Cell* **29**, 2106-2125. doi:10.1105/tpc.17.00099
- Costa, L. M., Marshall, E., Tesfaye, M., Silverstein, K. A. T., Mori, M., Umetsu, Y., Otterbach, S. L., Papareddy, R., Dickinson, H. G., Boutilier, K. et al. (2014). Central cell-derived peptides regulate early embryo patterning in flowering plants. *Science* **334**, 168-172. doi:10.1126/science.1243005
- Dobin, A., Davis, C. A., Schlesinger, F., Drenkow, J., Zaleski, C., Jha, S., Batut, P., Chaisson, M. and Gingeras, T. R. (2013). STAR: ultrafast universal RNA-Seq aligner. *Bioinformatics* **29**, 15-21. doi:10.1093/bioinformatics/bts635
- Dong, J., MacAlister, C. A. and Bergmann, D. C. (2009). BASL controls asymmetric cell division in *Arabidopsis*. *Cell* **137**, 1320-1330. doi:10.1016/j.cell.2009.04.018
- Haecker, A., Gross-Hardt, R., Geiges, B., Sarkar, A., Breuninger, H., Herrmann, M. and Laux, T. (2004). Expression dynamics of *WOX* genes mark cell fate decisions during early embryonic patterning in *Arabidopsis thaliana*. *Development* **131**, 657-668. doi:10.1242/dev.00963
- Hiei, Y., Ohta, S., Komari, T. and Kumashiro, T. (1994). Efficient transformation of rice (*Oryza sativa* L.) mediated by *Agrobacterium* and sequence analysis of the boundaries of the T-DNA. *Plant J.* **6**, 271-282. doi:10.1046/j.1365-313X.1994.6020271.x
- Hong, S.-K., Aoki, T., Kitano, H., Satoh, H. and Nagato, Y. (1995). Phenotypic diversity of 188 rice embryo mutants. *Dev. Genet.* **16**, 298-310. doi:10.1002/dvg.1020160403
- Itoh, J.-I., Sato, Y., Sato, Y., Hibara, K.-Y., Shimizu-Sato, S., Kobayashi, H., Takehisa, H., Sanguinet, K. A., Namiki, N. and Nagamura, Y. (2016). Genome-wide analysis of spatio-temporal gene expression patterns during early embryogenesis in rice. *Development* **143**, 1217-1227. doi:10.1242/dev.123661
- Jeong, S., Palmer, T. M. and Lukowitz, W. (2011). The RWP-RK factor *GROUNDED* promotes embryonic polarity by facilitating YODA MAP kinase signaling. *Curr. Biol.* **15**, 1268-1276. doi:10.1016/j.cub.2011.06.049
- Jürgens, G. (2001). Apical-basal patterning formation in *Arabidopsis* embryogenesis. *EMBO J.* **20**, 3609-3616. doi:10.1093/emboj/20.14.3609
- Kamiya, N., Nishimura, A., Sentoku, N., Takabe, E., Nagato, Y., Kitano, H. and Matsuoka, M. (2003). Rice *globular embryo4 (gle4)* mutant is defective in radial pattern formation during embryogenesis. *Plant Cell Physiol.* **44**, 875-883. doi:10.1093/pcp/pcg112
- Kishi-Kaboshi, M., Okada, K., Kurimoto, L., Murakami, S., Umezawa, T., Shibuya, N., Yamane, H., Miyao, A., Takatsuji, H., Takahashi, A. et al. (2010). A rice fungal MAMP-responsive MAPK cascade regulates metabolic flow to antimicrobial metabolite synthesis. *Plant J.* **63**, 599-612. doi:10.1111/j.1365-313X.2010.04264.x
- Kouchi, H. and Hata, S. (1993). Isolation and characterization of novel nodulin cDNAs representing genes expressed at early stages of soybean nodule development. *Mol. Gen. Genet.* **238**, 106-119.
- Liu, S., Hua, L., Dong, S., Chen, H., Zhu, X., Jiang, J., Zhang, F., Li, Y., Fang, X. and Chen, F. (2016). OsMAPK6, a mitogen-activated protein kinase, influences rice grain size and biomass production. *Plant J.* **84**, 672-681. doi:10.1111/tpj.13025
- López-Bucio, J. S., Dubrovsky, J. G., Raya-González, J., Ugartechea-Chirino, Y., López-Bucio, J., de Luna-Valdez, L. A., Ramos-Vega, M., León, P. and Guevara-García, A. A. (2014). *Arabidopsis thaliana* mitogen-activated protein kinase 6 is involved in seed formation and modulation of primary and lateral root development. *J. Ex. Bot.* **65**, 169-183. doi:10.1093/jxb/ert368
- Lukowitz, W., Roeder, A., Parmenter, D. and Somerville, C. (2004). A MAPKK kinase gene regulates extra-embryonic cell fate in *Arabidopsis*. *Cell* **116**, 109-119. doi:10.1016/S0092-8674(03)01067-5
- Mayer, U., Ruiz, R. A. T., Berleth, T., Miséra, S. and Jürgens, G. (1991). Mutations affecting body organization in the *Arabidopsis* embryo. *Nature* **353**, 402-407. doi:10.1038/353402a0
- Mikami, M., Toki, S. and Endo, M. (2015). Comparison of CRISPR/Cas9 expression constructs for efficient targeted mutagenesis in rice. *Plant Mol. Biol.* **88**, 561-572. doi:10.1007/s11103-015-0342-x
- Minkenbergh, B., Xie, K. and Yang, Y. (2017). Discovery of rice essential genes by characterizing a CRISPR-edited mutation of closely related MAP kinase genes. *Plant J.* **89**, 636-648. doi:10.1111/tpj.13399
- Miyao, A., Tanaka, K., Murata, K., Sawaki, H., Takeda, S., Abe, K., Shinozuka, Y., Onosato, K. and Hirochika, H. (2003). Target site specificity of the *Tos17* retrotransposon shows a preference for insertion within genes and against insertion in retrotransposon-rich regions of the genomes. *Plant Cell* **15**, 1771-1780. doi:10.1105/tpc.012559
- Nardmann, J., Zimmermann, R., Durantini, D., Kranz, E. and Werr, W. (2007). *WOX* gene phylogeny in *Poaceae*: a comparative approach addressing leaf and embryo development. *Mol. Biol. Evol.* **24**, 2474-2484. doi:10.1093/molbev/msm182
- Ohnishi, T., Yoshino, M., Yamakawa, H. and Kinoshita, T. (2011). The biotron breeding system: a rapid and reliable procedure for genetic studies and breeding in rice. *Plant Cell Physiol.* **52**, 1249-1257. doi:10.1093/pcp/pcr066
- Robinson, M. D., McCarthy, D. J. and Smyth, G. K. (2010). EdgeR: a bioconductor package for differential expression analysis of digital gene expression data. *Bioinformatics* **26**, 139-140. doi:10.1093/bioinformatics/btp616
- Sato, Y., Hong, S. K., Tagiri, A., Kitano, H., Yamamoto, N., Nagato, Y. and Matsuoka, M. (1996). A rice homeobox gene, *OSH1*, is expressed prior to organ differentiation in a specific region during early embryogenesis. *Proc. Natl. Acad. Sci. USA* **93**, 8117-8122. doi:10.1073/pnas.93.15.8117
- Smith, R. A. and Long, J. A. (2010). Control of *Arabidopsis* apical-basal embryo polarity by antagonistic transcription factors. *Nature* **464**, 423-426. doi:10.1038/nature08843
- Spinner, L., Gadeyne, A., Belcram, K., Goussot, M., Moison, M., Duroc, Y., Eeckhout, D., De Winne, N., Schaefer, E., Van De Slijke, E. et al. (2013). A protein phosphatase 2A complex spatially controls plant cell division. *Nat. Comm.* **4**, 1863. doi:10.1038/ncomms2831
- Takahashi, H., Kamakura, H., Sato, Y., Shiono, K., Abiko, T., Tsutsumi, N., Nagamura, Y., Nishizawa, N. K. and Nakazono, M. (2010). A method for obtaining high quality RNA from paraffin sections of plant tissues by laser microdissection. *J. Plant Res.* **123**, 807-813. doi:10.1007/s10265-010-0319-4
- Toki, S., Hara, N., Ono, K., Onodera, H., Tagiri, A., Oka, S. and Tanaka, H. (2016). Early infection of scutellum tissue with *Agrobacterium* allows high-speed transformation in rice. *Plant J.* **47**, 969-976. doi:10.1111/j.1365-313X.2006.02836.x
- Torres-Ruiz, R. A. and Jürgens, G. (1994). Mutations in the *FASS* gene uncouple pattern formation and morphogenesis in *Arabidopsis* development. *Development* **120**, 2967-2978.
- Ueda, M., Zhang, Z. and Laux, T. (2011). Transcriptional activation of *Arabidopsis* axis patterning genes *WOX8/9* links zygote polarity to embryo development. *Dev. Cell* **20**, 264-270. doi:10.1016/j.devcel.2011.01.009
- Ueda, M., Aichinger, E., Gong, W., Groot, E., Verstraeten, I., Vu, L. D., Smet, I. D., Higashiyama, T., Umeda, M. and Laux, T. (2017). Transcriptional integration of parental and maternal factors in the *Arabidopsis* zygote. *Genes Dev.* **31**, 617-627. doi:10.1101/gad.292409.116
- Vollbrecht, E. and Hake, S. (1995). Deficiency analysis of female gametogenesis in Maize. *Dev. Genet.* **16**, 44-63. doi:10.1002/dvg.1020160109
- Wang, H., Nhwanyama, N., Liu, Y., Walker, J. C. and Zhang, S. (2007). Stomatal development and patterning are regulated by environmentally responsive mitogen-activated protein kinase in *Arabidopsis*. *Plant Cell* **19**, 63-73. doi:10.1105/tpc.106.048298
- Wardlaw, C. W. (1955). Embryogenesis in flowering plants. In *Embryogenesis in Plants*, pp. 223-251. New York: Wiley & Sons.
- Yi, J., Lee, Y. S., Lee, D. Y., Cho, M. H., Jeon, J. S. and An, G. (2016). *OsMPK6* plays acritical role in cell differentiation during early embryogenesis in *Oryza sativa*. *J. Exp. Bot.* **67**, 2425-2437. doi:10.1093/jxb/erw052
- Yu, T.-Y., Shi, D.-Q., Jia, P.-F., Tang, J., Li, H.-J. and Yang, W.-C. (2016). The *Arabidopsis* Receptor kinase *ZAR1* is required for zygote asymmetric division and its daughter cell fate. *PLoS Genet.* **12**, e1005933. doi:10.1371/journal.pgen.1005933
- Zhang, X., Zong, J., Liu, J., Yin, J. and Zhang, D. (2010). Genome-wide analysis of *WOX* gene family in Rice, Sorghum, Maize, *Arabidopsis* and Poplar. *J. Int. Plant Biol.* **52**, 1016-1026. doi:10.1111/j.1744-7909.2010.00982.x
- Zhang, M., Wu, H., Su, J., Wang, H., Zhu, Q., Liu, Y., Xu, J., Lukowitz, W. and Zhang, S. (2017). Maternal control of embryogenesis by *MPK6* and its upstream *MKK4/5* in *Arabidopsis*. *Plant J.* **92**, 1005-1019. doi:10.1111/tpj.13737
- Zhao, P., Begcy, K., Dresselhaus, T. and Sun, M.-X. (2017). Does early embryogenesis in eudicots and monocots involve the same mechanism and molecular players? *Plant Physiol.* **173**, 130-142. doi:10.1104/pp.16.01406